Journal of Nano- and Electronic Physics
Vol. **12** No 4, 04008(7pp) (2020)

Журнал нано- та електронної фізики
Том **12** № 4, 04008(7cc) (2020)

Effect of pH on Structural Morphology and Magnetic Properties of Ordered Phase of Cobalt Doped Lithium Ferrite Nanoparticles Synthesized by Sol-gel Auto-combustion Method

L.S. Kaykan[1,*], J.S. Mazurenko[2], N.V. Ostapovych[2], A.K. Sijo[3], N.Ya. Ivanichok[4]

[1] *Vasyl Stefanyk Precarpathian National University, 57, Shevchenko St., 76018 Ivano-Frankivsk, Ukraine*
[2] *Ivano-Frankivsk National Medical University, 2, Halytska St., 76000 Ivano-Frankivsk, Ukraine*
[3] *Department of Physics, Mary Matha Arts and Science College, Manathavady, 670645 Kerala, India*
[4] *G.V. Kurdyumov Institute for Metal Physics of NAS of Ukraine, Kyiv, Ukraine*

(Received 16 April 2020; revised manuscript received 15 August 2020; published online 25 August 2020)

Cobalt doped lithium ferrite nanoparticles were synthesized at different pH by sol-gel method. The effect of pH on the physical properties of cobalt doped lithium ferrite nanoparticles has been investigated. The nanoparticles synthesized at different pH were characterized through X-ray diffraction (XRD), scanning electron microscopy (SEM), energy dispersive X-ray analysis (EDAX), Mossbauer spectroscopy and impedance spectroscopy. The XRD patterns were analyzed to determine the crystal phase of cobalt doped lithium ferrite nanoparticles synthesized at different pH. The results of XRD showed the formation of an unmixed cobalt-substituted lithium ferrite having an ordered phase of the spinel structure. SEM micrographs show that the structural morphology of the nanoparticles is highly sensitive to the pH during the synthesis process. The electrical properties of the nanoparticles were also investigated: conductivity, real and imaginary parts of the dielectric constant, loss tangent. These characteristics have been found to differ for nanoparticles synthesized at different pH values which may be caused by differences in the size and morphology of the nanoparticle surface.

Keywords: Sol-gel method, Cobalt substitution, Nanocrystalline ferrites, pH effect, X-ray diffraction, Magnetic properties.

DOI: 10.21272/jnep.12(4).04008

PACS numbers: 71.20.Nr, 72.15.Eb, 72.20.Pa, 77.22.Gm, 73.22. – f, 76.80. + y

1. INTRODUCTION

Spinel ferrites are unique materials that exhibit ferromagnetic and semiconductor properties and can be considered as magnetic semiconductors. These materials are widely used in a number of devices, including recording heads, antenna rods, recording devices, microwave devices, core materials for energy converters in electronic and telecommunication applications. Nanosized ferrites can have remarkable electrical and magnetic properties that are significantly different from microstructured materials, adaptable to modern technologies such as ferromagnetic fluids, magnetic transporters for drugs, high density information devices, photocatalysts, gas sensors, and so on [1]. There is growing interest in studying the effect of synthesis conditions on the morphology and properties of such materials.

Compared to other ferrite materials, lithium ferrites have one important feature: because lithium ions are combined with Fe^{3+} ions, the concentration of Fe^{2+} ions is reduced, which makes the material resistance very high.

For the synthesis of lithium ferrite nanoparticles, a number of methods are used, such as aqueous co-precipitation, sol-gel method, solid-state reaction method, hydrothermal, and others. Compared with other methods, the sol-gel method has several advantages, such as low process temperature, homogeneous distribution of reagents, the ability to obtain nanosized particles and great adaptability to the synthesis of nanocrystalline powders [4]. Finally, several studies on the synthesis and physical properties of lithium-cobalt ferrite nanoparticles are presented in [5-7]. However, in these publications there is no information on the effect of pH on the structural morphology and physical properties of cobalt-substituted lithium ferrites. Thus, the results of the synthesis of cobalt-substituted lithium ferrite nanoparticles at different pH values obtained by the sol-gel method using citric acid as a chelating agent are presented in this work. The effect of pH change on the structure, morphology and electrical properties of the synthesized nanoparticles was also investigated.

2. SYNTHESIS AND RESEARCH METHODS

2.1 Synthesis

Cobalt-substituted lithium ferrites were synthesized as follows: at the first stage of the synthesis, a stoichiometric amount of Li, Co and Fe aqueous nitrates and citric acid were mixed together into deionized water according to the compositional formula $Li_{0.2}Co_{0.6}Fe_{2.2}O_4$ to prepare 0.06 mol solution [8, 10]. The nitrates of metals and citric acid were mixed dropwise on a magnetic stirrer in a molar ratio of metals to citric acid 1:1.75. Then, the pH of the above prepared solution was maintained by adding the 25 % aqueous solution of ammonia. Finally, three systems with different pH values (3, 7, 9) were obtained. Mixture of metal nitrate-citric acid solutions was slowly evaporated within the temperature range of 70-80 °C to remove extra amount of water from the solutions. Further, the solutions were heated once again at 110 °C to

*larysa.kaykan@gmail.com

obtain a viscous gel and completely remove the adsorbed water. The obtained xerogel was placed in an oven, where it was heated to a temperature of about 200-220 °C after which the mixture ignited and the reaction formed a product that was investigated using an X-ray diffractometer DRON-3 in CuKα-radiation.

2.2 Research Methods

The obtained samples were characterized by a powder X-ray diffractometer [XRD, DRON-3] equipped with a copper target and nickel filter to examine the phase purity and crystallinity. X-ray wavelength used in the study was 0.15406 nm of CuKα operated at 30 kV and 30 mA.

Fig. 1 shows the dried gel and the product formed after burning.

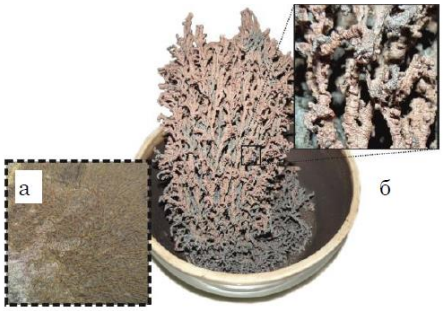

Fig. 1 – Synthesis of lithium-iron spinel by sol-gel autocombustion method: a) dried xerogel; b) the product formed after the reaction

For the analysis of the experimental diffraction patterns, the full-profile Rietveld method and the PowderCell program were used. ^{57}Fe absorption spectra were obtained using Mossbauer spectrometer MS1104EM. ^{57}Co was used as a γ-quanta source in chromium matrix with an activity value of 100 mCi. The decryption of the received spectra was carried out in the application package Univem with calibration. Investigation of electrical properties of samples was carried out using an impedance spectrometer Autolab PGSTAT 12/FRA-2 in the frequency range of 0.01 Hz-100 kHz. The surface morphology of the specimens was investigated using JSM-6700F scanning electron microscope at accelerating voltage of 15 kV.

Magnetic investigation was carried out using a vibration magnetometer 7407 VSM (Lake Shore Cryotronics).

Experimental magnetic moment for the formula unit m_{exp} measured in Bohr magnetons (μ_B) can be calculated using the formula

$$m_{\exp} = \frac{M_W M_S}{5585},$$

where M_W is a molecular weight of the sample and M_S is a saturation magnetization (emu/g).

The constant of magnetic anisotropy (K) can be expressed due to the saturation magnetization (M_S) and magnetic coercive force (H_c) [9] as

$$K = \frac{M_S H_c}{0.96}.$$

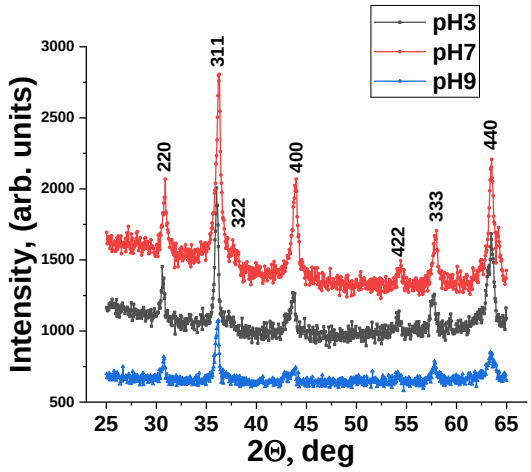

Fig. 2 – Experimental XRD patterns of the $Li_{0.2}Co_{0.6}Fe_{2.2}O_4$ system obtained at different pH values of the reaction media: pH = 3 (a); pH = 7 (b); pH = 9 (c)

3. RESULTS AND DISCUSSION

3.1 Structural Analysis and Morphology

Fig. 2 presents the X-ray diffraction (XRD) patterns of the synthesized compounds of the $Li_{0.2}Co_{0.6}Fe_{2.2}O_4$ composition obtained by the sol-gel method of autocombustion at pH values of the reaction medium equal to 3, 7 and 9 (i.e., in acidic, neutral and alkaline media).

Analysis of the diffractograms of all the synthesized samples indicates the presence of the inversed spinel phase of magnesium-substituted lithium ferrite with major diffraction planes (220), (311), (400), (422), (511) and (440) (JCPDS-38-0259). The plane (311) has the maximum value of the diffraction intensity, which is an indication that this direction is predominant. No diffraction peaks corresponding to other phases such as α-Fe_2O_3, CoO or nitro compounds of these elements were observed. Thus, based on the observations, it can be stated that the cobalt ions were completely replaced in the lithium ferrite lattice for all investigated pH values. The cationic distribution obtained from the analysis of experimental XRD patterns using the full-profile Rietveld method can be represented as $[Co_{0.32}Fe_{0.72}](Li_{0.2}Fe_{1.4}Co_{0.37})$. It can be seen that the Li^+ cations occupy only the B-positions, whereas the Fe^{3+} and Co^{2+} ions occupy both the A- and B-sites. Thus, cobalt-substituted lithium ferrite is a mixed spinel with a degree of inversion $\delta = 0.24$ and belongs to the spatial group Fd3m.

The dependence of the lattice constant on the pH of the reaction medium is shown in Fig. 3.

The sizes of coherent scattering regions (CSR) were determined by the Scherrer method

$$\langle D \rangle = \frac{\lambda}{\beta_{\frac{1}{2}} \cos\theta},$$

where λ is the wavelength of X-ray radiation, θ is the diffraction angle, $\beta_{1/2}$ is the half-width of reflection. Also CSR were determined by the Williamson-Hall interpolation method, according to which the dependence of $\beta\cos\theta$ on $\sin\theta$ was built based on the equation $\beta\cos\theta = \lambda/D + 4\varepsilon\sin\theta$ (if the approximation was per-

formed by Lorentz or Cauchy functions) or equation $\beta^2\cos^2\theta = (\lambda/D)^2 + (4\varepsilon\sin\theta)^2$ (if the approximation was carried out by the Gauss function). If obtained dependence is approximated linearly, then the angle of inclination of the line will be proportional to the magnitude of the micro-voltages (ε or ε^2), and the intersection of the line with the ordinate axis is the value inversely proportional to the size of the CSR (D or D^2). Table 1 shows the CSR size values for the $Li_{0.2}Co_{0.6}Fe_{2.2}O_4$ system at pH = 3, 7, 9 calculated by both methods.

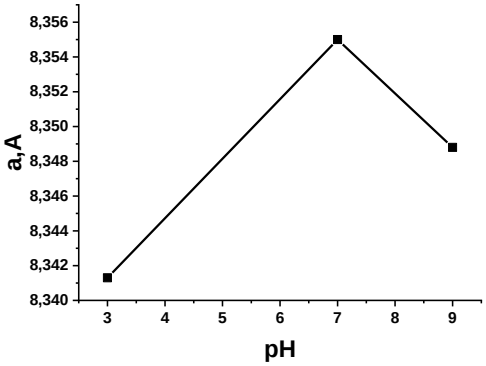

Fig. 3 – The dependence of the lattice constant on the pH of the reaction medium of the $Li_{0.2}Co_{0.6}Fe_{2.2}O_4$ system

Table 1 – CSR sizes for $Li_{0.2}Co_{0.6}Fe_{2.2}O_4$ system at different pH values of the reaction media

pH	CSR, nm The Selyakov-Scherrer method	CSR, nm Williamson-Hall method
3	30	28.5
7	20	19.0
9	25	23.4

The data in Table 1 indicate that all the synthesized samples are nanosized and the pH of the reaction medium plays a significant role in the formation of the microstructure of the synthesized samples. The somewhat larger CSR values in the Selyakov-Scherrer method are due to the fact that only one intensity peak (the third one) was taken into account, while the Williamson-Hall method takes into account all the reflexes. As it is known, as the angle of reflection increases, the half-width of the peak increases, so taking into account all the reflexes can give an average value that may be slightly smaller than that for one randomly selected reflex. Also when determining the magnitude of $\beta_{1/2}$ the instrumental widening caused by the X-ray beam divergence and the width of the limiting slit were taken into account; this was determined using a reference sample. This sample served as a well-annealed sample of lithium-iron spinel obtained in a ceramic way.

The effect of the pH of the reaction medium on the microstructure of the synthesized systems can be interpreted as follows: ammonia (NH_4OH) was added to establish the appropriate pH value in the precursor solution. Ammonia increases the chelation of metal cations with citrate [7], which can help control the oxygen balance [7] and promotes the formation of porous three-dimensional (3D) structure in nitrate-citrate xerogels [6]. Fe^{3+} has been found to be complete with citrate only when the pH is approximately 3 [7]. From this, we can conclude that without ammonia citric acid works only as a fuel. Insufficient chelation of metal ions with citrates can lead to imperfect 3D gel structure and thus the nitrate oxidant introduced into the xerogel can easily decompose both during the drying process and during the combustion process. This will reduce the amount of heat generated by the lack of oxidant so that the ferrite compound is formed as a result [7]. The optimum pH is 6 for spinel ferrite formation, as to Waqas et al. [6]. It was also found that with increasing pH to 6, the decomposition of citric acid contained in xerogel occurs at 220 °C in one stage and, as a result, a single-phase spinel ferrite is formed. The decomposition of citrate-nitrate xerogel without ammonia fully occurs only at 500 °C. Nitrate-citrate xerogels without ammonia flash locally and, as a result, amorphous powder is formed. Xerogels obtained from a solution at pH > 7 interfere with the process of spontaneous flare, thus, even when forming a single-phase structure of ferrite, its morphology is quite dense and, as a result, the formed system is characterized by higher values of CSR. However, in most studies on the synthesis of ferrite spinel from nitrate-citrate gels, pH values equal to 7 were chosen. Yue and others found that when the pH is greater than 4, a crystallized phase NH_4NO_3 occurs, which decomposes into NH_3, NO_x and H_2O during the drying process and, as a result of gassing, 3D xerogel structure forms. For pH = 2 and 3, the gel detects a dense mesh microstructure, in which there are only single pores in the gel structure. If the pH value is increased, a mesh structure develops in the gel. At pH = 6 and 7, 3D mesh structure is fully formed. Due to the porous mesh structure, more oxygen is introduced into the xerogel. Oxygen accelerates the combustion process, thus increasing the combustion temperature and speed. The porous structure makes xerogel burning fast and very strong. Moreover, the NH_4NO_3 decomposition is accompanied by the release of O_2, thus accelerating the combustion process. High pH values of the solution mixture are desirable for the synthesis of ferrite compounds with increased values of initial magnetic permeability. At the same time, with increasing pH, the size of crystallites increases, which is an attribute of a higher combustion temperature [5].

The X-ray density of the synthesized compounds was calculated by the ratio

$$d_x = \frac{ZM}{Na^3},$$

where Z is the number of molecules per unit cell (for the spinel lattice $Z = 8$), M is the mass of the ferrite sample molecule, N is the Avogadro number, and a is the lattice constant.

At pH = 7, the X-ray density has a minimum. This is obviously due to the fact that under these conditions of synthesis (the reaction medium is neutral), the combustion process is most intensive at high speed. As a result, the particles do not have time to agglomerate, resulting in a fine powder with crystallite sizes smaller than 20 nm. Accordingly, for such specimens, the influence of the surface is strongly manifested and, as a result, the lattice constant increases, which in turn leads to a decrease in the X-ray density.

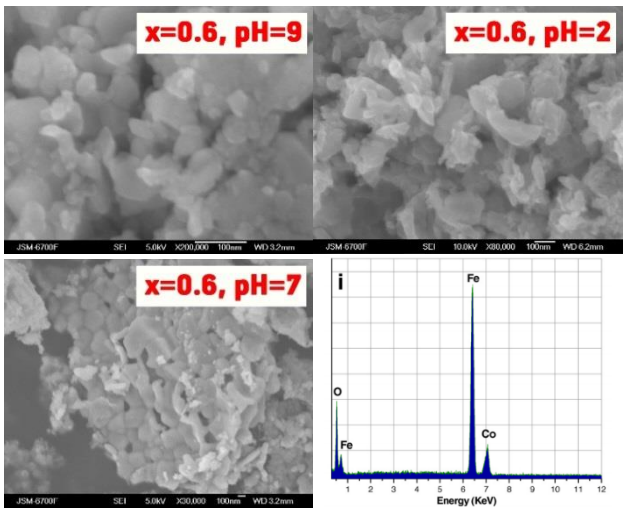

Fig. 4 – Typical scanning electron microscopic (SEM) images and EDAX spectra of $Li_{0.2}Co_{0.6}Fe_{2.2}O_4$ obtained at different pH values of the reaction medium (pH = 3, 7, 9)

3.2 Mossbauer Studies

Mossbauer spectra of ^{57}Fe at room temperature of $Li_{0.2}Co_{0.6}Fe_{2.2}O_4$ obtained at different pH values of the reaction medium (pH = 7) are shown at Fig. 6.

All spectra obtained are a superposition of two sextets corresponding to the A and B positions of iron in spinel sublattices. The values of the magnetic fields are 490 and 447 kE, respectively. Table 2 shows the main parameters of the Mössbauer spectra of $Li_{0.2}Co_{0.6}Fe_{2.2}O_4$ systems synthesized at different pH values of the reaction medium.

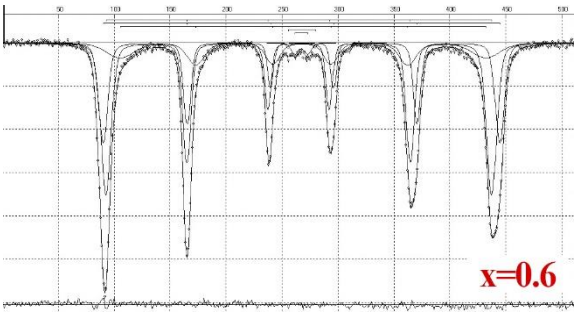

Fig. 5 – Mössbauer spectra of ^{57}Fe at room temperature of the $Li_{0.2}Co_{0.6}Fe_{2.2}O_4$ system obtained at different pH values of the reaction medium (pH = 7)

Table 2 – Parameters for decoding the Mössbauer spectra of $Li_{0.2}Co_{0.6}Fe_{2.2}O_4$ nanoparticles synthesized at different pH

pH value		*Is*, mm/s	*Qs*, mm/s	*H*, koE	*S*, %	*G*, mm/s
3	1st sextet	0.295	0.078	447.51	34.82	0.840
	2nd sextet	0.295	0.022	490.75	23.73	0.469
	doublet	0.306	0.640	–	41.44	0.7982
7	1st sextet	0.220	0.040	440.00	20.12	0.766
	2nd sextet	0.306	– 0.008	489.75	35.60	0.530
	doublet	0.313	0.660	–	44.28	0.695
9	1st sextet	0.233	0.059	442.01	24.42	0.772
	2nd sextet	0.301	– 0.006	490.24	40.17	0.568
	doublet	0.311	0.653	–	35.40	0.692

3.3 Conductive and Dielectric Properties

Dielectric constant (ε') and dielectric loss (ε'') were obtained depending on the change in the pH of the reaction medium in the process of synthesis by the sol-gel autocombustion method. Dependences of ε' and ε'' on frequencies at pH values of 2, 7, 9 are shown in Fig. 6. It was discovered that both ε' and ε'' increase with increasing frequency, but the nature of the change is strongly dependent on the pH level. Thus, the features of frequency dependences of ε' and ε'' can be induced by polarization effects caused by the change in morphology during synthesis at different pH of the reaction medium. A number of authors [3, 5] have shown that the mechanism of dielectric polarization is similar to the conductivity mechanism, confirming that the result of interaction in the exchange of electrons leads to a local displacement of electrons in the direction of the electric field, which determines the polarization of ferrite. The change in spatial polarization is determined by both the amount of space charge carriers and the presence of defects between phase or inter-particle boundaries. As shown by the results of XRD and morphological studies, deviation of the pH of the reaction medium in any direction from neutral (pH = 7) leads to a decrease in the thermal output of the reactions and, as a consequence, to an increase in the reaction time. This, in turn, leads to an increase in the size of the crystallites and a decrease in the partial contribution of the boundaries of the section. Obviously, this is the main reason for the differences in the electrical properties of the identical composition.

3.4 Magnetic Measurements

Magnetic measurements were performed on samples synthesized at different pH values of the reaction medium 2, 7 and 9, which correspond to the acidic, neutral and alkaline synthesis medium. Initially, measurements were made in ZFC conditions with the applied magnetic field (B) of 1 T from 300 K to 1200 K. Magnetization measurements (M) on B were performed at 300 K. Thus, FC measurements were carried out from 1200 K to 300 K in the applied 1 T magnetic field.

Fig. 7 shows the dependence of the magnetic susceptibility on the temperature for the sample synthesized at pH 7. The dependence for other pH values has a similar behavior, but it is worth noting the increase in the initial values (M), which can obviously be explained by the differences in morphology, that is, the increase in particle size. This assumption was also confirmed by X-ray analysis and electron microscopy data.

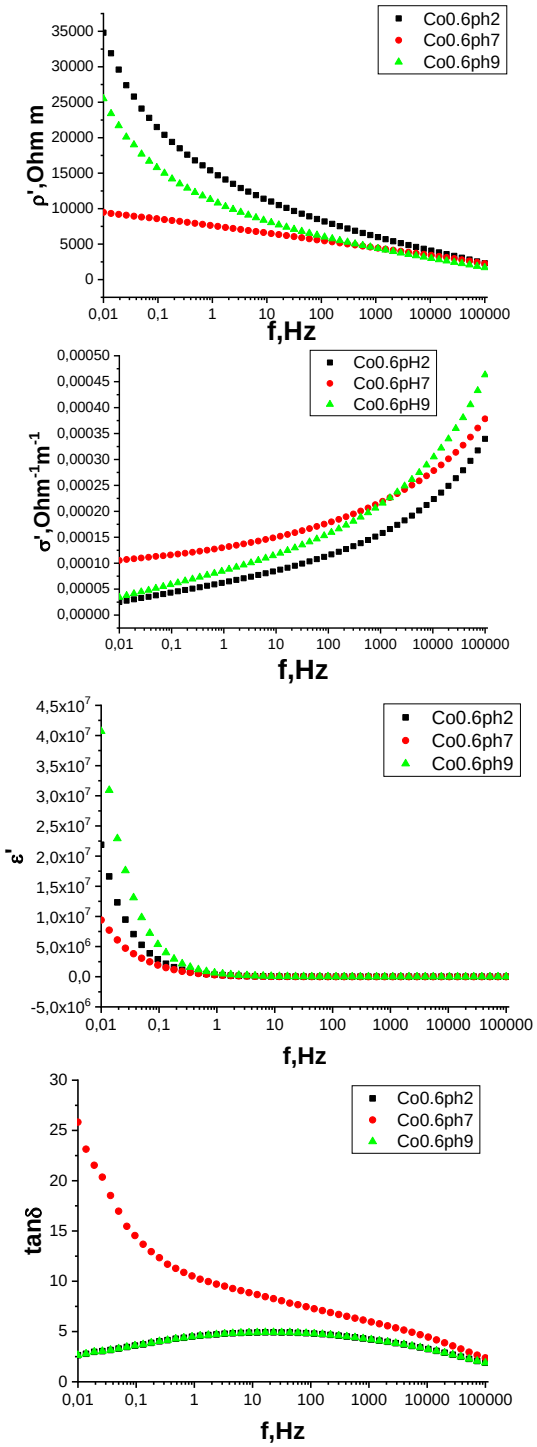

Fig. 6 – Frequency dependences of the electrical parameters $\rho'(f)$, $\sigma'(f)$, $\varepsilon'(f)$, $\tan\delta(f)$ at different pH values

Fig. 8 shows the temperature dependence of the derivative of the magnetic susceptibility. As can be seen from the figure, deviations of the heating mode at temperatures 749, 830 and 1030 K are observed. This characterizes the change in the structure of the ferromagnetic material. In this case, at 749 K, the lattice is transformed from an ordered to a disordered state due to the influence of the induced temperature factor on the phonon spectrum of the original sample. 1030 K is the phase transition temperature of the ferromagnetic-paramagnetic state.

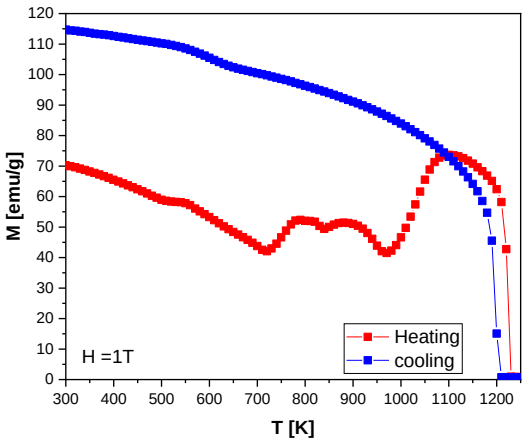

Fig. 7 – The dependence of the magnetic susceptibility on the temperature obtained by heating the sample and cooling at H = 1 T in the temperature range of 300-1200 K

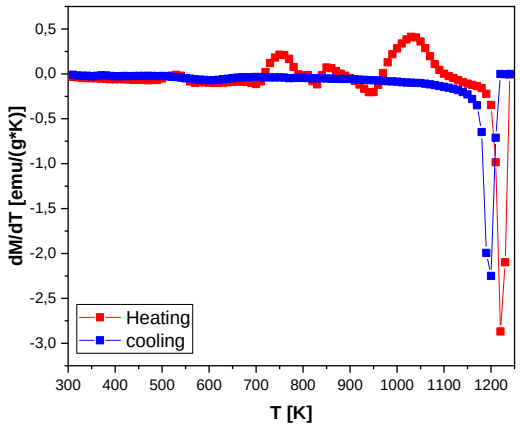

Fig. 8 – Temperature dependence of the derivative of the magnetic susceptibility of the system synthesized at pH = 7

Samples synthesized at pH = 2 have the highest magnetic susceptibility. Obviously, this can be explained by the fact that these samples have the greatest value of CSR.

Fig. 9 shows the magnetization curves before heating at 300 K and after cooling at 300 K.

As noted earlier from the XRD data, samples synthesized at different pH values of the reaction medium are characterized by a single phase of lithium ferrite (Fig. 2). SEM images of these samples (Fig. 4) showed an increase in grain sizes varying from 100 nm for the sample obtained at pH = 7 to 4 μm for the sample synthesized at pH = 2. This indicates an increase in the probability of random distribution of magnetic moments, and therefore an increase in its magnetic quality.

Table 3 shows the main magnetic characteristics of cobalt-substituted lithium-iron ferrite synthesized at different pH values of the reaction medium.

In literature [3, 6, 9], the magnetization of lithium ferrites is about 60 emu/g, which is lower than the values obtained in this paper (Table 3). In these samples, the increase in saturation magnetization is caused by the substitution of magnetic ions (cobalt), as well as, as mentioned above, by the difference in the morphology of the samples synthesized at different pH values.

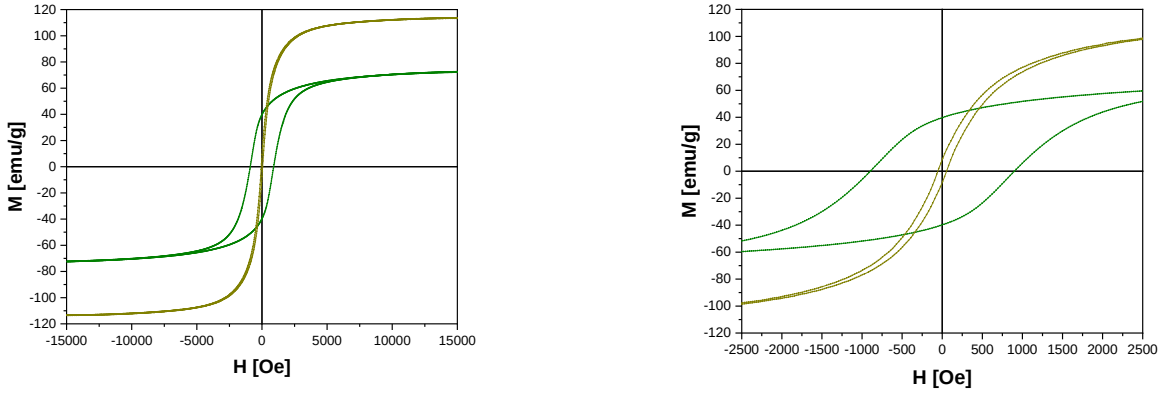

Fig. 9 – Dependences of magnetization on magnetic field before heating and after cooling at 300 K (a); enlarged area near zero (b)

Table 3 – Magnetic characteristics of cobalt-substituted lithium-iron ferrite synthesized at different pH of the reaction medium

pH of the reaction medium	Molar mass μ	Coercivity Hc	Remnant magnetization Mr	Saturation magnetization Ms	Anisotropic constant $K \times 10^4$	Magnetic moment m_{ef}
2	223.5	902	37	75.2	7.1	3.00
7	223.5	888.5	39.9	72.23	6.9	2.89
9	223.5	890	35	73.3	6.8	2.93
measurement errors	± 0.01	± 0.1	± 0.01	± 0.01	0.01	± 0.01

ACKNOWLEDGEMENTS

Authors acknowledge faculty of Physical Engineering, Igor Sikorsky Kyiv Polytechnic Institute National Technical University of Ukraine for X-ray measurements; Faculty of Physics and Technology, Vasyl Stefanyk Precarpathian National University, Ukraine for Mössbauer measurements and Laboratory of Magnetometry, Rzeszow University of Technology, Rzeszow, Poland for SEM measurements.

REFERENCES

1. O.M. Uhorchuk, V.V. Uhorchuk, M.V. Karpets, L.S. Kaykan, B.Ja. Deputat, A.M. Boychuk, M.I. Hasyuk, *J. Nano- Electron. Phys.* **7** No 2, 02012 (2015).
2. J. Liu, Y. Mei, W. Liu, *J. Magn. Magn. Mater.* **454**, 6 (2018).
3. L.S. Kaykan, J.S. Mazurenko, *J. Nano- Electron. Phys.* **11** No 5, 05041 (2019).
4. J. Uday Bhasker, G. Narsinga Rao, *J. Magn. Magn. Mater.* **452**, 398 (2018).
5. A.K. Sijo, Vikash Kumar Jha, *J. Magn. Magn. Mater.* **497**, 166047 (2020).
6. Md.D. Rahaman, T. Nusrat, R. Maleque, *J. Magn. Magn. Mater.* **451**, 391 (2018).
7. L. Sun, J. Guo, R. Zhang, *J. Magn. Magn. Mater.* **449**, 545 (2017).
8. B.K. Ostafiychuk, L.S. Kaykan, *Nanoscale. Res. Lett.* **12**, 237 (2017).
9. A.K. Sijo, *J. Magn. Magn. Mater.* **441**, 672 (2017).
10. L.S. Kaykan, J.S. Mazurenko, A.K. Sijo, V.I. Makovysyn, *Appl. Nanosci.* (2020).

Вплив pH на морфологію структури і магнітні властивості впорядкованої фази наночастинок кобальт-заміщеного літієвого фериту, синтезованого золь-гель методом

Л.С. Кайкан[1], Ю.С. Мазуренко[2], Н.В. Остапович[2], A.K. Sijo[3], Н.Я. Іванічок[4]

[1] *ДВНЗ "Прикарпатський національний університет імені Василя Стефаника", вул. Шевченка, 57, 76018 Івано-Франківськ, Україна*
[2] *Івано-Франківський національний медичний університет, вул. Галицька, 2, 76000 Івано-Франківськ, Україна*
[3] *Department of Physics, Mary Matha Arts and Science College, Manathavady, 670645 Kerala, India*
[4] *Інститут металофізики імені Г.В. Курдюмова НАН України, Київ, Україна*

Наночастинки кобальт-заміщеного літієвого фериту були синтезовані при різних pH методом золь-гель автоспалювання. Було досліджено вплив pH на структуру, морфологію, електричні та магнітні властивості наночастинок кобальт-заміщеного літієвого фериту. Наночастинки, синтезовані при різних pH, досліджувалися методами рентгенівської дифракції (XRD), скануючої електронної спектроскопії (SEM), енергодисперсійного рентгенівського аналізу (EDAX), мессбауерівської та імпедансної спектроскопії. Рентгенівські дифрактограми аналізувалися для визначення кристалічної фази наночастинок кобальт-заміщеного літієвого фериту, синтезованого при різних pH. Результати рентгенівської дифракції показали формування бездомішкового кобальт-заміщеного літієвого фериту, що має впорядковану фазу шпінельної структури. SEM зображення показали, що морфологія структури на-

ночастинок сильно залежить від pH реакційного середовища в процесі синтезу. Енергодисперсійний рентгенівський аналіз підтвердив очікуваний хімічний склад синтезованого продукту. Мессбауерівські спектри систем, синтезованих при різних значеннях pH реакційного середовища, також суттєво відрізняються один від одного. Показано, що катіонний розподіл чинить значний вплив на значення ізомерного зсуву і величини надобмінних полів заліза, що знаходяться в тетра- і октаоточенні. Також досліджувалися електричні властивості наночастинок: провідність, дійсна та уявна частини діелектричної проникності, тангенс втрат, і виявилося, що вони відрізняються для наночастинок, синтезованих при різних pH, що може бути викликано відмінностями в розмірах та морфології поверхні наночастинок. Дослідження магнітних властивостей синтезованих порошків за допомогою вібраційного магнетометра (7407 VSM (Lake Shore Cryotronics)) показали сильну залежність магнітних параметрів від рівня pH реакційного середовища при отриманні досліджуваних феритів. Значення намагніченості насичення немонотонно залежить від вмісту іонів кобальту і має вище значення порівняно з частинками, отриманими іншими способами. Виявлена однозначна кореляція між рівнем pH реакційного середовища, розміром отриманих частинок і фізичними параметрами досліджуваних систем.

Ключові слова: Ферити, Золь-гель автоспалювання, Рентгенівська дифракція, Заміщення кобальту, Нанокристалічні ферити, pH-ефект, Магнітні властивості.